Relevance of complex branch points for partial wave analysis

S. Ceci,[1] M. Döring,[2] C. Hanhart,[3,4] S. Krewald,[3,4] U.-G. Meißner,[2,3,4] and A. Švarc[1]

[1]*Rudjer Bošković Institute, Bijenička 54, HR-10000 Zagreb, Croatia*
[2]*HISKP (Theorie), Universität Bonn, Nußallee 14-16, D-53115 Bonn, Germany*
[3]*Institut für Kernphysik and Jülich Center for Hadron Physics, Forschungszentrum Jülich, D-52425 Jülich, Germany*
[4]*Institute for Advanced Simulation, Forschungszentrum Jülich, D-52425 Jülich, Germany*

A central issue in hadron spectroscopy is to deduce—and interpret—resonance parameters, namely, pole positions and residues, from experimental data, for those are the quantities to be compared to lattice QCD or model calculations. However, not every structure in the observables derives from a resonance pole: the origin might as well be branch points, either located on the real axis (when a new channel composed of stable particles opens) or in the complex plane (when at least one of the intermediate particles is unstable). In this paper we demonstrate first the existence of such branch points in the complex plane and then show on the example of the πN P_{11} partial wave that it is not possible to distinguish the structures induced by the latter from a true pole signal based on elastic data alone.

I. INTRODUCTION

The second and third resonance region of baryonic excited states is currently under intense experimental investigation at various laboratories such as ELSA, MAMI, and JLab [1–4]. Many resonances overlap at these energies, and usually partial wave analyses in different frameworks, such as K-matrix approaches or dynamical coupled-channel models [5–23], are necessary to disentangle the resonance content. Furthermore, many resonances may couple only weakly to the πN channel, and the investigation of different initial and final states in hadronic reactions is mandatory [19]. Also, at these energies multipion intermediate and final states are becoming increasingly important and should be included in the analysis of the S matrix. For the corresponding T matrix, channels with stable particles like ηN induce a branch point at the threshold energy ($\sqrt{s} = m_\eta + M_N$), which may be visible as a cusp in the amplitude [24,25].

For effective multipion channels with one unstable and one stable particle, such as ρN, the analytic structure is more complicated. In comparison to the branch points on the real s axis and the first and second sheet poles, the third type of allowed singularities is given by branch points within the complex energy plane. They emerge when amongst groups of particles of an at least three-body decay there exists a strong correlation between two particles. For example, a significant fraction of $\pi^+\pi^- X$ intermediate and final states typically goes through the ρ meson. The resulting line shapes are discussed in Ref. [26]. Branch points in the complex plane also emerge in the recently developed complex-mass scheme for baryonic resonances [27].

Known theoretically for a long time [28,29], these branch points are present in several modern approaches, such as the GWU/SAID analysis [5,6], the Jülich [15–19] and EBAC [21,22] approaches, and the Bonn-Gatchina [14] analysis. It is the goal of this study to demonstrate the model-independent character of these complex branch points. To do so, we employ

general properties of the S matrix only. In a particular example it is then shown that the branch points are of relevance in partial wave analyses: if the theoretical partial wave does not include them, their absence can easily be simulated by resonance poles. This, of course, distorts the extracted baryon spectrum. Branch points in the complex plane are thus important for the reliable extraction of resonance parameters.

The paper is organized as follows: in Sec. II the existence of branch points in the complex plane is derived from three-body phase space, in Sec. II A the properties of the branch points are determined, and in Sec. III it is shown that these branch points are relevant in the extraction of the resonance content of partial waves.

II. ANALYTIC STRUCTURE OF THE S MATRIX AND COMPLEX BRANCH POINTS

Every channel opening introduces a new branch point and with it a new sheet to the S matrix, located at $s = (\sum m_i)^2$, with m_i being the masses of the stable particles in that channel. The first sheet is always the physical one, i.e., where the physical amplitude is situated. The only singularities allowed on the first sheet are poles on the real s axis below the lowest threshold (= bound states) or branch points on the real axis. On other sheets, poles and branch points can be located anywhere. Poles on the second sheet are called resonances if their real part is located above the lowest threshold, and they are called virtual states if they are located below the threshold, but on the real axis. It is also possible to have poles on the second sheet inside the complex plane with a real part lower than the threshold [30] or on other hidden sheets that are often referred to as shadow poles.

In this study we are interested in branch points on the second sheet in the complex plane, i.e., on the same sheet on which the resonance poles are situated. To prove the emergence of these branch points, let us start from the optical

theorem

$$
T(j \to i) - T^\dagger(j \to i)
$$
$$
= i(2\pi)^4 \sum_f \int d\Phi_f\, T^\dagger(i \to f) T(j \to f), \quad (1)
$$

where $T(j \to i)$ denotes the T matrix connecting channels i and j and $d\Phi_f$ denotes the phase space of channel f. To simplify the argument we assume that the T matrix is in a particular partial wave; below we focus on the singularities that stem from the unitarity cuts only. Singularities like the left-hand cuts, the short nucleon cut [18,31], or the circular cut, induced by the partial wave projection, are ignored in the following for they are irrelevant for the argument given.

To be specific we use the normalization of phase space as proposed by the Particle Data Group [32]. Then we have the following for the n-particle phase space,

$$
d\Phi_n(P; p_1, \ldots, p_n) = \delta^{(4)}\left(P - \sum_i p_i\right) \prod_i \frac{d^3 p_i}{(2\pi)^3 2E_i}, \quad (2)
$$

where P is the overall center-of-mass (c.m.) four-momentum.

To avoid complications, which are irrelevant for the validity of the present argumentation, we now focus on the diagonal channel $i = j$. To be concrete we assume $i = \pi N$. To further simplify the argument, in addition, we focus on $f = \rho N$ as the only relevant intermediate $\pi\pi N$ channel. The latter assumption allows us to write

$$
T(\pi N \to \pi\pi N) = i\, W(m_{\pi\pi}^2) D(m_{\pi\pi}^2) T(\pi N \to \rho N), \quad (3)
$$

where $D(m_{\pi\pi}^2)$ denotes the physical ρ propagator as a function of the $\pi\pi$ invariant mass $m_{\pi\pi}$ and $W(m_{\pi\pi}^2)$ is the partial wave projected decay vertex, which contains also the information on the orbital angular momentum ℓ of the decay into $\pi\pi$. In the following we abbreviate $m \equiv m_{\pi\pi}$.

One can decompose the three-body phase space into two subspaces [32],

$$
d\Phi_n(P; p_1, \ldots, p_n)
$$
$$
= d\Phi_j(q; p_1, \ldots, p_j)
$$
$$
\times d\Phi_{n-j+1}(P; q, p_{j+1}, \ldots, p_n)(2\pi)^3 dm^2. \quad (4)
$$

For the example of the $\rho[\pi\pi]N$ system considered here, the first factor $d\Phi$ refers to the $\pi\pi$ phase space in the ρ subsystem at four-momentum q (note that $m^2 = q^2$), the second is the ρN phase space at four-momentum P, and $n = 3$ and $j = 2$. With this decomposition,

$$
\int d\Phi_j(q; p_1, \ldots, p_j)|D(m^2) W(m^2)|^2 = -\frac{1}{\pi} \mathrm{Im}[D(m^2)]
$$
$$
= \rho(m^2), \quad (5)
$$

where $\rho(m^2)$ denotes the spectral density for the resonance normalized via

$$
\int_{4m_\pi^2}^\infty dm^2 \rho(m^2) = 1. \quad (6)
$$

We get for the discontinuity of the πN amplitude from the $\pi\pi N$ channel

$$
\frac{1}{i}[T(\pi N \to \pi N) - T^\dagger(\pi N \to \pi N)]
$$
$$
= (2\pi)^7 \int dm^2 \rho(m^2) \int d\Phi_2(P; q, p_3)
$$
$$
\times |T(\pi N \to \rho N)(s, m^2)|^2 + \ldots, \quad (7)
$$

where the ellipses denote contributions from the other channels omitted here. The two-body phase space can be calculated explicitly. One finds

$$
d\Phi_2(P; q, p_3) = \frac{1}{256\pi^6} \frac{p(\sqrt{s}, m, m_3)}{\sqrt{s}} d\Omega, \quad (8)
$$

with

$$
p(\sqrt{s}, m, m_3) = \frac{1}{2\sqrt{s}} \sqrt{[s - (m_3 + m)^2)(s - (m_3 - m)^2]}
$$
$$
(9)
$$

for the c.m. momentum of the nucleon (particle 3) and the pion pair with invariant mass m.

Using Eq. (7) we may thus express the T matrix through a dispersion integral and obtain

$$
T(\pi N \to \pi N)
$$
$$
= \frac{1}{4} \int_{(M_N + 2m_\pi)^2}^\infty \frac{ds'}{\sqrt{s'}} \int_{4m_\pi^2}^{(\sqrt{s'} - M_N)^2} dm^2\, \rho(m^2)\, p(\sqrt{s'}, m, m_3)
$$
$$
\times \int d\Omega \frac{|T(\pi N \to \rho N)(s', m^2)|^2}{s' - s + i\epsilon} + \ldots, \quad (10)
$$

where now the ellipses stand for the unitarity cut contributions from other channels as well as left-hand cut contributions. First of all, there is the three-body cut, which drives the inelasticity of the T matrix. To be concrete, we may write

$$
\rho(m^2) = -\frac{N}{\pi} \mathrm{Im} \frac{1}{m^2 - m_\rho^2 + i m_\rho \tilde\Gamma},
$$
$$
\tilde\Gamma = \Gamma \frac{\tilde p(m, m_\pi, m_\pi)^{2\ell+1}}{p_0^{2\ell+1}}, \quad (11)
$$

where p_0 is the three-momentum at the nominal resonance mass and N is a normalization factor so that Eq. (6) is fulfilled. The factor $(\tilde p/p_0)^{2\ell+1}$ accounts for the centrifugal barrier and $\tilde p$ is the pion momentum in the ρ rest frame. Note, $\tilde p = p(m, m_\pi, m_\pi)$ at the $\pi\pi N$ threshold ($\sqrt{s} = 2m_\pi + M_N$); i.e., the ρ is at rest and the ρ rest frame and the overall rest frame coincide. Note also that the explicit form of Eq. (11) is only for illustration. The m dependence of the denominator is more complicated in general (see, e.g., the Appendix), but the only property needed in the following is the presence of poles in the spectral function.

Indeed, the spectral function $\rho(m^2)$ of Eq. (11) contains a pair of poles located at $m^2 = m_0^2$, where m_0 denotes the pole position of the ρ meson, located in the complex plane. We may write $m_0 = m_\rho \pm i\Gamma/2$, where Γ denotes the width of the ρ meson.

For the existence of branch points in the complex plane, it is sufficient to consider the imaginary part of Eq. (10) in
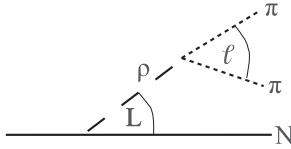
FIG. 1. The quasiparticle (ρ) coupling to the stable particle N with orbital angular momentum L; the decay of the quasiparticle into stable particles (2π) is in ℓ wave with respect to the quasiparticle c.m. frame.

the following, or, more correctly, we consider the analytic function δT, which is $\delta T = \operatorname{Im} T$ for $\sqrt{s} \in \mathbb{R}$, but of course $\delta T \neq \operatorname{Im} T$ for $\sqrt{s} \notin \mathbb{R}$ (e.g., δT develops an imaginary part for complex $\sqrt{s}$, whereas $\operatorname{Im} T$ does not). The function δT can be straightforwardly evaluated,

$$\delta T = -\frac{\pi}{4\sqrt{s}} \int_{4m_\pi^2}^{(\sqrt{s}-M_N)^2} dm^2 \, \rho(m^2)$$
$$\times p(\sqrt{s}, m, M_N) \, p(\sqrt{s}, m, M_N)^{2L} \, g(\sqrt{s}, m), \quad (12)$$

with p from Eq. (9). In Eq. (12), we have explicitly denoted a factor of p^{2L} that comes from the $L = 0, 1, \ldots$ transition $T(\pi N \to \rho N)$. The function $g(\sqrt{s}, m)$ contains the integral $\int d\Omega$ over the part of $|T|^2$ without these centrifugal barrier factors. In general, $g(m + M_N, m) \neq 0$. The overall process we consider here as an example is shown in Fig. 1.

A function $f(\sqrt{s})$ has a branch point z_b at $\sqrt{s} = z_b$, whenever in its integral representation $f(\sqrt{s}) = \int_a^b dq \, \tilde{f}(\sqrt{s}, q)$ the function $\tilde{f}$ has a simple pole at $q = q_0$ and a $\sqrt{s} = z_b$ exists such that $q_0 = a$ or $q_0 = b$. For example, the integrand of the two-body phase space integral $\int_0^\infty dq \, q^2/(\sqrt{s} - E_1 - E_2 + i\epsilon)$, where $E_i = \sqrt{m_i^2 + q^2}$, has a simple pole at $q_0 = p(\sqrt{s}, m_1, m_2)$ with the on-shell momentum p from Eq. (9). Then, the branch point is given for the $\sqrt{s}$ for which $q_0 = 0$ (lower integration limit). This is the case for $\sqrt{s} \equiv z_b = m_1 + m_2$, i.e., the branch point is at the two-body threshold.

With this knowledge, it is straightforward to determine the branch points of δT: as discussed before, the simple poles of the integrand (spectral function) are located at the complex $m^2 = m_0^2$ which equals the upper integration limit of Eq. (12) for $\sqrt{s} = M_N + m_0$.

Thus, without loss of generality, we have shown that poles in the spectral function at $m = m_0$ lead to branch points of the amplitude at the complex scattering energy $\sqrt{s} = M_N + m_0$ or

$$\sqrt{s} \equiv z_{b1,2} = M_N + m_\rho \pm i\Gamma/2. \quad (13)$$

More generally, the model-independent result is that z_b is given by the sum of the mass of the stable particle plus m_0, where m_0 is the pole position in the scattering amplitude of the subsystem, in this case given by $\pi\pi$ which resonates through a ρ meson. Equation (13) has also been obtained in Ref. [18], starting from an explicit expression for the $\pi\pi N$ system, derived from field theory, and in which the $\pi\pi$ subsystem is boosted. In Appendix A we will come back to the connection of that formalism to the present one.
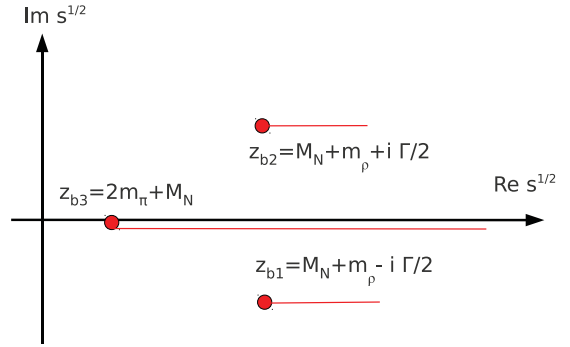

FIG. 2. (Color online) Analytic structure of the amplitude. There are three branch points z_{b1}, $z_{b2} = z_{b1}^*$, and z_{b3}. z_{b1} and z_{b2} are structures in δT and thus on the second sheet.

The branch points z_b in Eq. (13) have been obtained by considering the upper integration limit in Eq. (12). However, also the lower integration limit can coincide with a singularity for a certain $\sqrt{s}$: this is the case for

$$\sqrt{s} \equiv z_{b3} = 2m_\pi + m_N, \quad (14)$$

for which the lower integration limit coincides with the branch point singularity coming from the factors of p in the integrand. The overall analytic structure is shown in Fig. 2. The first, physical sheet has the branch point z_{b3} with an associated cut. If the cut is chosen along the real $\sqrt{s}$ axis like in the figure, the discontinuity of the amplitude is given by $2\,\delta T$ from Eq. (12). The branch points z_{b1} and z_{b2} are in δT, i.e., on the sheet that is obtained by analytically continuing the discontinuity of the first sheet. They are, thus, on the second sheet, where also resonance poles are normally situated. The branch points z_{b1} and z_{b2} induce the new sheets 3 and 4; they are analytically connected to the second sheet along the cuts induced by z_{b1} and z_{b2}. In Fig. 2 these cuts are chosen parallel to the real $\sqrt{s}$ axis; in Ref. [18] they are chosen parallel to the imaginary $\sqrt{s}$ axis, which is a convenient choice to search for poles. For the numbering of sheets, see also Ref. [18].

A. Threshold behavior

Apart from determining the existence and position of branch points, one can also deduce their threshold behavior, i.e., the functional form of δT close to the three z_b's. In Fig. 1, the three-body decay is schematically shown. Let the quasiparticle (ρ) couple to the stable particle (N) in L wave in the overall c.m. system, while the quasiparticle decays into stable particles (two pions) in ℓ wave with respect to the quasiparticle c.m. frame.

In the following we use the explicit form of Eq. (11) to determine the threshold behavior. It is clear, however, that the final results do not depend on this particular form for the spectral function, but only on the fact that the spectral function has poles [right side of Eq. (15)] and the presence of factors of p in Eq. (12) that follow from the previously given phase space derivation.

To study the behavior of the amplitude in the complex energy plane close to the branch points $z_{b1,2}$, complex values

of m^2 will be needed, and thus the (nonanalytic) function Im in Eq. (11) needs to be evaluated to obtain a meromorphic expression,

$$\rho(m^2) = \frac{N}{\pi} \frac{m_\rho \tilde{\Gamma}}{(m^2 - m_\rho^2)^2 + m_\rho^2 \tilde{\Gamma}^2} \xrightarrow{m \to m_0} \frac{\Gamma h_1(m^2)}{m^2 - m_0^2} . \quad (15)$$

The right-hand side shows the behavior of $\rho(m^2)$ close to the pole at $m = m_0$; the function h_1 does not contain any poles or zeros close to m_0 and thus does not influence the threshold behavior. In particular, $\tilde{p}^{2\ell+1}$, which appears in the numerator [cf. Eq. (11)], has no zero close to m_0 and can be absorbed in h_1. Thus the threshold behavior of the branch points z_{b1} and z_{b2} does not depend on ℓ, which may appear to be a surprising result.

To obtain the threshold behavior of the branch points z_{b1} and z_{b2} in the complex plane, one inserts the right-hand side of Eq. (15) into Eq. (12),

$$\delta T \sim \int_{4m_\pi^2}^{(\sqrt{s} - M_N)^2} dm^2 \frac{\Gamma \left(m^2 - m_0^2\right)^{\frac{2L+1}{2}} h_2(m^2)}{m^2 - m_0^2}, \quad (16)$$

where we have expanded the argument of the square root of the p factors of Eq. (12) in m^2, at the point $p(\sqrt{s} = z_b = M_N + m_0, m, M_N)$ to obtain the power of the leading zero from these factors. The function h_2 is again analytic, free of zeros close to $m = m_0$, and does not influence the threshold behavior. The integral may now be evaluated setting this numerator and h_2 constant. The result for the threshold behavior of the branch points z_{b1} and z_{b2} is [see also Eq. (13)]

$$\delta T(z_{b1,2}) \sim \left(\sqrt{s} - z_{b1,2}\right)^{\frac{2L+1}{2}} \sim p(\sqrt{s}, m_0, M_N)^{2L+1}. \quad (17)$$

In Fig. 3 we show the branch point z_{b2} in the upper $\sqrt{s}$ half plane [see Fig. 2] for a realistic ρN intermediate state and $L = 0$. The branch point is clearly visible, together with the cut that in this picture is chosen in the positive Re $\sqrt{s}$ direction.

To obtain the threshold behavior for the third branch point at $z_{b3} = 2m_\pi + M_N$ (see Fig. 2), we inspect again Eq. (15). As discussed following Eq. (11), close to $\sqrt{s} = z_{b3} = 2m_\pi + M_N$ [see Eq. (14)] the ρ c.m. frame coincides with the overall c.m. frame, i.e., $\tilde{p} = p(m, m_\pi, m_\pi)$, and thus the ℓ-wave decay in the ρ subsystem is also an ℓ-wave decay in the overall c.m. system. For $\sqrt{s}$ in the vicinity of z_{b3}, the denominator of Eq. (15) is free of zeros; however, in contrast to the case of z_{b1} and z_{b2}, the numerator $\tilde{\Gamma} \sim \tilde{p}^{2\ell+1} = p^{2\ell+1} = (m^2 - 4m_\pi^2)^{(2\ell+1)/2}$ does have a zero that contributes to the threshold behavior. Inserting Eq. (15) (including this factor) in Eq. (12) and expanding the arguments of the square roots of the p factors around zero [cf. Eq. (9)], one obtains

$$\delta T \sim \int_{4m_\pi^2}^{(\sqrt{s} - M_N)^2} dm^2 \Gamma \left(m^2 - 4m_\pi^2\right)^{\frac{2\ell+1}{2}}$$
$$\times \left(m^2 - 4m_\pi^2\right)^{\frac{2L+1}{2}} h_3(m^2), \quad (18)$$

with a function h_3 free of zeros and poles in the vicinity of z_{b3}. Integration leads now to the threshold behavior
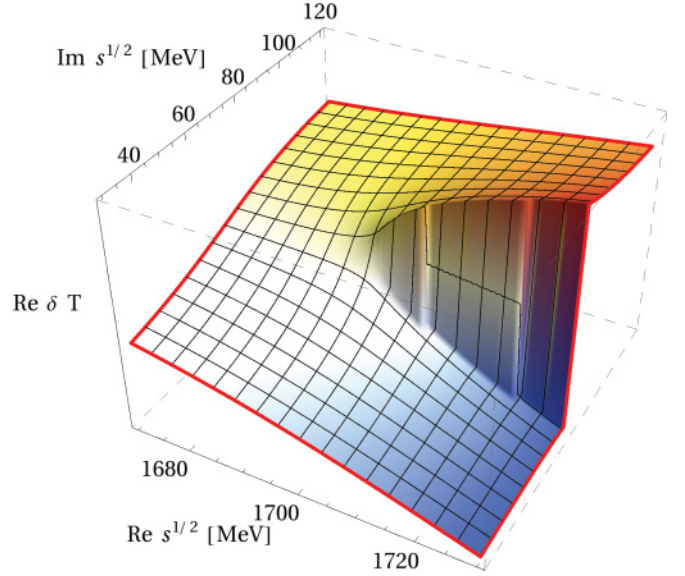

FIG. 3. (Color online) Branch point z_{b2} in Re δT in the upper $\sqrt{s}$ half plane, for a realistic ρN intermediate state. The cut is chosen here in the positive Re $\sqrt{s}$ direction.

of z_{b3},

$$\delta T(z_{b3}) \sim [\sqrt{s} - (2m_\pi + M_N)]^{\ell+L+2}$$
$$\sim p(\sqrt{s}, M_N, 2m_\pi)^{2\ell+2L+4} . \quad (19)$$

This corresponds to the opening of the three-body threshold. Note that even if $\ell = L = 0$, the threshold behavior is still $\sim p^4$, i.e., the standard three-body phase space; thus, this threshold opening is always smooth.

B. The limit of vanishing width

It is instructive to study the limit of a vanishing width of the ρ meson in Eq. (7). Then

$$\rho(m^2) \longrightarrow \delta\left(m^2 - m_\rho^2\right) \quad \text{for} \quad \Gamma \to 0.$$

This allows us to perform the m^2 integration to get

$$\frac{1}{i}[T(\pi N \to \pi N) - T^\dagger(\pi N \to \pi N)]$$
$$= (2\pi)^7 \Theta[(\sqrt{s} - M_N)^2 - m_\rho^2] \int d\Phi_2(P; q, p_3)$$
$$\times \left|T(\pi N \to \rho N)(s, m_\rho^2)\right|^2 + \dots, \quad (20)$$

such that Eq. (10) reduces to the dispersion integral over the standard two-body cut

$$T(\pi N \to \pi N) \to \frac{1}{4} \int_{(M_N + m_\rho)^2}^{\infty} \frac{ds'}{\sqrt{s'}} p(\sqrt{s'}, m_\rho, M_N)$$
$$\times \int d\Omega \frac{\left|T(\pi N \to \rho N)(s', m_\rho^2)\right|^2}{s' - s + i\epsilon} + \dots. \quad (21)$$

The imaginary part, which is given by

$$\delta T_{\Gamma \to 0} = -\pi/(4\sqrt{s}) \, p(\sqrt{s}, m_\rho, M_N)^{2L+1} g(\sqrt{s}, m_\rho), \quad (22)$$

has a branch point at $\sqrt{s} = m_\rho + M_N$, which is simply the ordinary two-body threshold on the real $\sqrt{s}$ axis. As $\Gamma \to 0$, the two branch points z_{b1} and z_{b2} in the complex plane move toward the real $\sqrt{s}$ axis until they coincide and form this single branch point at $\sqrt{s} = m_\rho + M_N$. Note that there is a factor of Γ in the numerator of Eq. (16), but in the limit $\Gamma \to 0$, another factor $\sim\Gamma$ appears in the denominators from the two poles moving to the real axis, which cancels the Γ of the numerator. Thus, indeed the branch point persists in the limit $\Gamma \to 0$ with the result given in Eq. (22).

For the third branch point at $z_{b3} = 2m_\pi + M_N$, Eq. (18) shows that there are no poles that can prevent the term from disappearing in the limit $\Gamma \to 0$; thus, as $\Gamma \to 0$, the third branch point fades away. In other words, $\Gamma \to 0$ means that the ρ decouples from $\pi\pi$ and, thus, in our example, the $\pi\pi N$ channel decouples from πN.

III. THE RELEVANCE OF BRANCH POINTS IN THE COMPLEX PLANE

As shown in the previous section, whenever there is a multiparticle intermediate state with pairwise strong correlations, unavoidably branch points show up in the complex plane. As we demonstrate on a particular example in this section, their influence on the data might well be visible. However, as will be also shown, it is in general not possible to deduce the origin of such a structure from elastic data only.

The first model we use is the so-called Jülich model [15–19]. It is a coupled-channel meson-exchange model including the channels πN, ηN, $K\Lambda$, and $K\Sigma$ as well as three effective $\pi\pi N$ channels, namely, $\pi\Delta$, σN, and ρN. All these two-pion channels show the mentioned kind of branch points [18]. In the Appendix we show the connection of the formalism of the Jülich model to the one of the previous section. The Jülich model allows for a good description of the available πN data in all partial waves with $j \leqslant 3/2$ up to an energy of 1.8 GeV and has been recently extended to higher energies, partial waves, and additional reactions [19].

To be specific we focus here on the P_{11} partial wave and the region around $\sqrt{s} \sim 1.7$ GeV. In this energy region, around 300 MeV above the Roper resonance, signals for another resonance, $N(1710)P_{11}$, have been found in several analyses [32]. It is, however, remarkable that in recent analyses of the GWU/SAID group [6], there is no sign for this resonance any more. Like the GWU/SAID analysis, the Jülich model contains explicitly the branch points z_{b1} and z_{b2} in the complex plane at $\sqrt{s} = M_N + m_\rho \pm i\,\Gamma/2 \sim 1700 \pm 75\,i$ MeV. However, there are no poles around these energies (the only genuine pole term in the P_{11} partial wave is the nucleon, while the poles of the Roper resonance are dynamically generated [15]). For the purpose of this study we have slightly changed the parameters of the model compared to the results of Ref. [16] to obtain a good description of the GWU/SAID solution. This is shown in Fig. 4 by the dashed lines. The important point here is that the theoretical amplitude in the complex plane around $\sqrt{s} \sim 1.7$ GeV is free of poles, but there is the ρN branch point.

To illustrate the difficulties in determining the origin of structures in the amplitude we fit this Jülich model amplitude
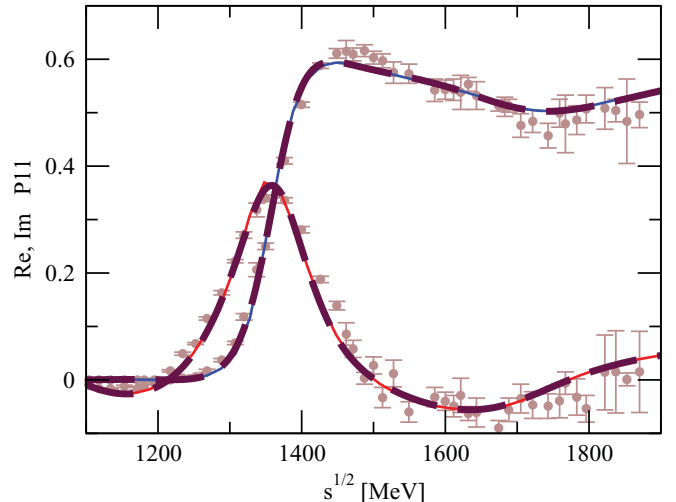

FIG. 4. (Color online) Fit of the CMB Zagreb model (solid lines) to the P_{11} amplitude provided by the Jülich model (dashed lines). The "data" points represent the single energy solution of the GWU/SAID group [6].

with another model, which does not contain the ρN branch point in the complex plane. For this, we use a Carnegie-Mellon-Berkeley (CMB) type of model that has been developed by the Zagreb group [8,9,33,34]. In this unitary coupled-channel model which respects analyticity, background plus resonances are provided, but all branch points are on the real axis. The result of the fit, using two resonance terms, is shown in Fig. 4 by the solid lines. As the figure shows, the fit is very precise and, in particular, shows no visible discrepancy to the amplitude of the Jülich model in the energy range shown.

However, the behavior in the complex plane is quite different: as mentioned before, there is no complex branch point in the CMB fit by construction; instead, a pole is found at $1698 - 130\,i$ MeV, which in this case might simulate the branch point missing in that model.

Thus, at a realistic scale of precision, the ρN branch point does not manifest itself in a unique structure on the physical axis; it can be simulated by resonance terms that produce poles in the complex plane. Still, the ρN branch point is a required structure of the S matrix, as shown in this study, and we have demonstrated that, in an analysis of partial waves, this and other branch points have to be included to avoid false resonance signals, which of course can totally distort the spectrum of excited baryonic resonances.

In such circumstances, one clearly has to consider other final states in which the resonance candidate shows a clearer signal. As already proposed in Ref. [35], performing global analyses of many different reaction channels within one theoretical ansatz is a much cleaner way to determine the resonance spectrum than increasing the precision of a partial wave for one reaction.

First steps within the coupled-channel Jülich model have been undertaken in this direction through the inclusion of some ρN data [15], ηN data [16], and, most recently, $K^+\Sigma^+$ data [19]. For the isospin $I = 1/2$ sector, we expect the inclusion

of $K^0\Lambda$ data to further clarify the role of the $N(1710)P_{11}$ (see also Ref. [36]).

Thus, the aim of the present short exercise is not to discard the existence of the much-debated $N(1710)P_{11}$ as such. Rather, we have shown that branch points in the complex plane are relevant; in their absence, resonances may be needed to simulate them, and, thus, the extracted baryon spectrum can be easily distorted.

IV. CONCLUSIONS

Using only general properties of the S matrix we have shown the existence and determined the position of three branch points induced by intermediate quasi-two-body states. Those are three-body states in which two particles are so strongly correlated that the scattering amplitude of this subsystem has a pole. A pole in the subsystem necessarily leads to the appearance of branch points in the complex $\sqrt{s}$ plane of the overall πN amplitude. This result is model independent because it does not depend on any particular parametrization, but only on analyticity and general properties of the three-body phase space. We have also determined the threshold behavior of all branch points, which depends on the orbital angular momenta of the two decay processes involved. Finally, on the example of the P_{11} partial wave, it has been shown that branch points in the complex plane are relevant in partial wave analysis: if a theoretical amplitude does not contain the branch points, false resonance signals may be obtained. To allow for a reliable extraction of the baryon spectrum, it is thus mandatory to include also these branch points in the analysis.

APPENDIX: SPECTRAL REPRESENTATION OF THE JÜLICH MODEL

In this appendix the connection of the field theoretical formalism, used in the Jülich model of hadron exchange, to the formalism used in this study is outlined, up to overall normalization factors. For further details of the formalism used in the Jülich model, we refer to Ref. [18]. For the example of the ρN propagator that is considered here, the propagator on the real axis is given by

$$g_{\rho N}(\sqrt{s}, k) = \frac{1}{\sqrt{s} - E_N(k) - E_\rho^0(k) - \Sigma[z_\rho(\sqrt{s}, k), k]},$$
(A1)

where E_N is the nucleon energy, E_ρ^0 is the ρ energy using the bare ρ mass, and Σ is the ρ self-energy, where $z_\rho(\sqrt{s}, k)$ is the boosted energy for the ρ subsystem. The explicit form of $z_\rho(\sqrt{s}, k)$ is quoted in Ref. [18] but for the present discussion the only needed property is that $z_\rho(\sqrt{s}, k = 0) = \sqrt{s} - M_N$. The propagator $g_{\rho N}$ is iterated in the multichannel scattering equation, but to investigate the analytic structure it is sufficient to consider the one-loop amplitude

$$G_{\rho N}(\sqrt{s}) = \int_0^\infty dk\, k^2\, g_{\rho N}(\sqrt{s}, k),$$
(A2)

where for simplicity we have omitted the form factors that regularize this divergent expression. One can rewrite the Dyson-Schwinger representation of Eq. (A1) with the spectral function

$$S(\omega, k) = -\frac{1}{\pi} \,\mathrm{Im}\, \frac{1}{\omega - E_N(k) - E_\rho^0(k) - \Sigma[z_\rho(\omega, k), k]},$$
(A3)

resulting in the Lehmann representation

$$g_{\rho N}(\sqrt{s}, k) = \int_{2m_\pi + M_N}^\infty d\omega\, \frac{S(\omega, k)}{\sqrt{s} - \omega + i\epsilon}.$$
(A4)

For the imaginary part of the ρN loop $G_{\rho N}(\sqrt{s})$, one obtains

$$\mathrm{Im}\, G_{\rho N}(\sqrt{s}) = \mathrm{Im}\, \int_0^\infty dk\, k^2\, g_{\rho N}(\sqrt{s}, k)$$
$$= -\pi \int_0^\infty dk\, k^2\, S(\sqrt{s}, k)$$
$$= -\pi \int_0^{k_1} dk\, k^2\, S(\sqrt{s}, k).$$
(A5)

The last equality shows that the integration can be cut at $k = k_1$ as for $k > k_1$ the spectral function is zero because then $z_\rho(\sqrt{s}, k) < 2m_\pi$. In particular, k_1 is given by $z_\rho(\sqrt{s}, k_1) = 2m_\pi$. Note that the explicit evaluation of the integration limits as done here is necessary if one wants to use the spectral representation in the complex $\sqrt{s}$ plane. This has been shown recently in the context of Feynman parametrized loops [37]: the integration limits have to be analytically continued for complex $\sqrt{s}$ to obtain the analytic continuation of the loop itself, and for this they need to be known explicitly.

Equation (A5) can be rewritten as

$$\mathrm{Im}\, G_{\rho N}(\sqrt{s}) = \int_{m_1}^{\sqrt{s} - m_\pi} dm\, \frac{S[\sqrt{s}, k^{\mathrm{on}}(m)]\, m}{E_m^{\mathrm{on}}}$$
$$\times (-\pi)\, \frac{k^{\mathrm{on}}(m)\, E_\pi^{\mathrm{on}}\, E_m^{\mathrm{on}}}{\sqrt{s}},$$
(A6)

with

$$k^{\mathrm{on}}(m) = p(\sqrt{s}, m, m_\pi), \quad E_\pi^{\mathrm{on}} = \sqrt{m_\pi^2 + (k^{\mathrm{on}})^2},$$
$$E_m^{\mathrm{on}} = \sqrt{m^2 + (k^{\mathrm{on}})^2},$$
(A7)

and p from Eq. (9). The lower integration limit m_1 is given as the solution of $z_\rho[\sqrt{s}, k^{\mathrm{on}}(m_1)] = 2m_\pi$. The second fraction in Eq. (A6) can be compared to the imaginary part of the well-known [18] propagator of two stable particles, M

and N,

$$\text{Im}\, G_{\text{stable}} = -\pi \, \frac{k^{\text{on}}(m=\sqrt{s})\, E_M^{\text{on}}\, E_N^{\text{on}}}{\sqrt{s}} \,. \qquad \text{(A8)}$$

Thus, the imaginary part of a loop with one stable and one unstable particle can be expressed as an integral over a distribution of imaginary parts of the form of Eq. (A8). Comparing Eq. (A6) to Eq. (12), one sees the formal similarity: there is an integral of a spectral function, which has poles [cf. Eq. (A3)], together with the factor $k^{\text{on}}(m) = p(\sqrt{s}, m, m_\pi)$, and both ingredients produce the three branch points z_{b1}, z_{b2}, and z_{b3} as has been shown in the main text (we have omitted here the additional $2L$ powers of p for simplicity). There is a difference in the chosen parametrization in terms of the spectral function [compare $p(\sqrt{s}, m, m_\pi)$ in Eq. (A7) vs $p(\sqrt{s}, m, M_N)$ in Eq. (12)], but this does not change the position of the branch points.

Indeed, $k^{\text{on}} = 0$ for the upper integration limit $m = \sqrt{s} - m_\pi$ and thus $z_\rho(\sqrt{s}, 0) = \sqrt{s} - M_N$. The poles of the ρ resonance in the spectral function S are located at the complex $z_\rho = z_\rho^0$ and consequently the integration limit equals the pole

position for $\sqrt{s} \equiv z_{b1,2} = M_N + z_\rho^0$, which is indeed Eq. (13). The singularity at $k^{\text{on}} = 0$, coming from the factor $k^{\text{on}}(m)$ in Eq. (A6), is also reached if $m = \sqrt{s} - m_\pi$. It is easy to show that this m equals the lower integration limit m_1 for $\sqrt{s} = 2m_\pi + M_N$ and thus Eq. (A6) indeed provides also the third branch point z_{b3} from Eq. (14).

In Ref. [18], the amplitude has been analytically continued to the complex plane using contour deformation. In fact, one could use the representation of Eq. (A6) for the same purpose in principle. As shown in the main text, for this, one has to respect the analyticity of the spectral function, i.e., the Im function in Eq. (A3) needs to be explicitly evaluated like in Eq. (15). Second, and this is an additional complication, the self-energy Σ itself has a two-sheet structure and the corresponding cut needs to be rotated as specified in Ref. [18]. This cut in Σ induces the cut of branch point z_{b3} in the overall πN amplitude. Apart from this and a carefully chosen integration path for the m integration of Eq. (A6), there are no additional complications, and the spectral representation allows for an alternative method of analytic continuation.

[1] E. Klempt and J. M. Richard, Rev. Mod. Phys. **82**, 1095 (2010).

[2] N. Sparks *et al.* (CBELSA/TAPS Collaboration), Phys. Rev. C **81**, 065210 (2010).

[3] J. Ahrens *et al.*, Phys. Rev. C **74**, 045204 (2006).

[4] I. Aznauryan, V. D. Burkert, T. S. Lee, and V. Mokeev, arXiv:1102.0597 [nucl-ex].

[5] R. A. Arndt, W. J. Briscoe, I. I. Strakovsky, and R. L. Workman, Phys. Rev. C **74**, 045205 (2006).

[6] R. Arndt, W. Briscoe, I. Strakovsky, and R. Workman, Eur. Phys. J. A **35**, 311 (2008).

[7] M. Batinić, I. Šlaus, A. Švarc, and B. M. K. Nefkens, Phys. Rev. C **51**, 2310 (1995).

[8] M. Batinić, I. Šlaus, A. Švarc, and B. M. K. Nefkens, Phys. Rev. C **57**, 1004(C) (1998).

[9] M. Batinić, I. Dadic, I. Šlaus, A. Švarc, B. M. K. Nefkens, and T. S. H. Lee, arXiv:nucl-th/9703023.

[10] D. Drechsel, S. S. Kamalov, and L. Tiator, Eur. Phys. J. A **34**, 69 (2007).

[11] R. L. Workman, M. W. Paris, W. J. Briscoe, L. Tiator, S. Schumann, M. Ostrick, and S. S. Kamalov, arXiv:1102.4897 [nucl-th].

[12] G. Penner and U. Mosel, Phys. Rev. C **66**, 055211 (2002).

[13] V. Shklyar, H. Lenske, and U. Mosel, Phys. Rev. C **72**, 015210 (2005).

[14] A. V. Anisovich, E. Klempt, V. A. Nikonov, A. V. Sarantsev, and U. Thoma, Eur. Phys. J. A **47**, 27 (2011).

[15] O. Krehl, C. Hanhart, C. Krewald, and J. Speth, Phys. Rev. C **62**, 025207 (2000).

[16] A. M. Gasparyan, J. Haidenbauer, C. Hanhart, and J. Speth, Phys. Rev. C **68**, 045207 (2003).

[17] M. Döring, C. Hanhart, F. Huang, S. Krewald, and U.-G. Meißner, Phys. Lett. B **681**, 26 (2009).

[18] M. Döring, C. Hanhart, F. Huang, S. Krewald, and U.-G. Meißner, Nucl. Phys. A **829**, 170 (2009).

[19] M. Döring, C. Hanhart, F. Huang, S. Krewald, U.-G. Meißner, and D. Rönchen, Nucl. Phys. A **851**, 58 (2011).

[20] M. W. Paris, Phys. Rev. C **79**, 025208 (2009).

[21] B. Juliá Díaz, T. S. H. Lee, A. Matsuyama, and T. Sato, Phys. Rev. C **76**, 065201 (2007).

[22] N. Suzuki, B. Juliá Díaz, H. Kamano, T. S. H. Lee, A. Matsuyama, and T. Sato, Phys. Rev. Lett. **104**, 042302 (2010).

[23] L. Tiator, S. S. Kamalov, S. Ceci, G. Y. Chen, D. Drechsel, A. Švarc, and S. N. Yang, Phys. Rev. C **82**, 055203 (2010).

[24] M. Döring and K. Nakayama, Eur. Phys. J. A **43**, 83 (2010).

[25] M. Döring and K. Nakayama, Phys. Lett. B **683**, 145 (2010).

[26] C. Hanhart, Yu. S. Kalashnikova, and A. V. Nefediev, Phys. Rev. D **81**, 094028 (2010).

[27] D. Djukanovic, J. Gegelia, and S. Scherer, Phys. Lett. B **690**, 123 (2010).

[28] W. R. Frazier and A. W. Hendry, Phys. Rev. **134**, B1307 (1964).

[29] R. E. Cutkosky and S. Wang, Phys. Rev. D **42**, 235 (1990).

[30] C. Hanhart, J. R. Pelaez, and G. Rios, Phys. Rev. Lett. **100**, 152001 (2008).

[31] G. Höhler, in *Pion Nucleon Scattering*, edited by H. Schopper, Landolt Börnstein, New Series, Group 9b, Vol. I (Springer, New York, 1983).

[32] K. Nakamura *et al.* (Particle Data Group), J. Phys. G **37**, 075021 (2010).

[33] M. Batinić, I. Dadic, I. Šlaus, A. Švarc, B. M. K. Nefkens, and T. S. H. Lee, Phys. Scr. **58**, 15 (1998).

[34] M. Batinić, S. Ceci, A. Švarc, and B. Zauner, Phys. Rev. C **82**, 038203 (2010).

[35] A. Švarc, S. Ceci, and B. Zauner, in *Proceedings of the Workshop on the Physics of Excited Nucleons NSTAR2005*, edited by S. Capstick, V. Crede, and P. Eugenio (World Scientific, Singapore, 2006), p. 37.

[36] S. Ceci, A. Švarc, and B. Zauner, Phys. Rev. Lett. **97**, 062002 (2006).

[37] M. Döring, D. Jido, and E. Oset, Eur. Phys. J. A **45**, 319 (2010).